MNRAS 000, 1–6 (2019) Preprint 16 October 2019 Compiled using MNRAS LATEX style file v3.0

Stellar feedback sets the universal acceleration scale in galaxies

Michael Y. Grudić[1,3]★, Michael Boylan-Kolchin[2], Claude-André Faucher-Giguère[1], and Philip F. Hopkins[3]

[1]*Department of Physics and Astronomy and CIERA, Northwestern University, 2145 Sheridan Road, Evanston, IL 60208, USA*
[2]*Department of Astronomy, The University of Texas at Austin, 2515 Speedway, Stop C1400, Austin, TX 78712, USA*
[3]*TAPIR, Mailcode 350-17, California Institute of Technology, Pasadena, CA 91125, USA*

Accepted XXX. Received YYY; in original form ZZZ

ABSTRACT

It has been established for decades that rotation curves deviate from the Newtonian gravity expectation given baryons alone below a characteristic acceleration scale $g_\dagger \sim 10^{-8}\,\mathrm{cm\,s^{-2}}$, a scale promoted to a new fundamental constant in MOND-type theories. In recent years, theoretical and observational studies have shown that the star formation efficiency (SFE) of dense gas scales with surface density, $\mathrm{SFE} \sim \Sigma/\Sigma_{\rm crit}$ with $\Sigma_{\rm crit} \sim (\dot{p}/m_*)/(\pi^2 G) \sim 1000\,\mathrm{M_\odot\,pc^{-2}}$ (where $\dot{p}/m_*$ is the momentum flux output by stellar feedback per unit stellar mass formed). We show that the star formation efficiency, more correctly, scales with the gravitational acceleration, i.e. that $\mathrm{SFE} \sim g_{\rm tot}/g_{\rm crit} \equiv (G\,M_{\rm enc}/R^2)/([\dot{p}/m_*]/\pi)$, where $M_{\rm enc}(<r)$ is the total gravitating mass and $g_{\rm crit} = (\dot{p}/m_*)/\pi = \pi\,G\,\Sigma_{\rm crit} \approx 10^{-8}\,\mathrm{cm\,s^{-2}} \approx g_\dagger$. It follows that the characteristic galactic acceleration $g_\dagger$ corresponds to the acceleration scale above which SF is 'efficient' (and outflows 'inefficient'), and so baryons inevitably dominate the mass. This also explains the "deep MOND" scaling $g_{\rm obs} \sim (g_{\rm baryon}\,g_\dagger)^{1/2}$ (where $g_{\rm baryon}$ is the acceleration due to baryons alone) apparent at low accelerations. We further show that $g_\dagger$ can be expressed in terms of fundamental constants (gravitational constant, proton mass, and Thomson cross-section): $g_\dagger \sim 0.1\,G\,m_p/\sigma_{\rm T}$.

Key words: galaxies: formation – galaxies: evolution – cosmology: dark matter

1 INTRODUCTION

The kinematics of galaxies require something beyond the Newtonian gravity of baryonic matter (e.g., Rubin et al. 1978, 1980; Bosma 1981a,b), an amazing observation that has moved from controversial to iron-clad over the past five decades (e.g., Bershady et al. 2011). In conjunction with observations of the cosmic microwave background and large-scale structure of the Universe (e.g., Planck Collaboration et al. 2018), this observation has led to the commonly-accepted idea that the mass content of the Universe is dominated by dark matter. In the standard Λ cold dark matter (ΛCDM) cosmology, dark matter reconciles observations with the fact that, according to general relativity, Newtonian gravity should be valid throughout the Universe whenever gravitational fields are weak (i.e., not in the immediate vicinity of compact objects such as black holes).

It is nevertheless curious within this model that the effects of dark matter appear not at a characteristic radius within galaxies, nor at a characteristic total mass, but rather at a critical *acceleration* scale. For gravitational accelerations $g \gg g_\dagger \approx 1.2\times10^{-8}\,\mathrm{cm\,s^{-2}}$, baryons dominate the gravitational dynamics of galaxies, while for $g \ll g_\dagger$, dark matter dominates. This observation led Milgrom (1983a,b,c) to propose that modifying Newton's law of gravity (or inertia) in the regime of very small accelerations, rather than the introduction of dark matter, is the correct interpretation of galaxy dynamics. More recently, Lelli et al. (2017) have shown that the total gravitational acceleration in disk galaxies is approximately predicted by the acceleration provided by the baryons alone, with the acceleration scale $g_\dagger$ providing the transition point above which the observed acceleration is given solely by that of the baryons and below which some additional acceleration is required.

Several groups have argued that this "Radial Acceleration Relation" (RAR) is a natural outcome of ΛCDM simulations (Keller & Wadsley 2017; Navarro et al. 2017; Ludlow et al. 2017; Dutton et al. 2019), but it is not immediately obvious *why*. In the context of ΛCDM, it is clear that something must connect the baryonic content of a disk galaxy

★ E-mail: mike.grudic@northwestern.edu

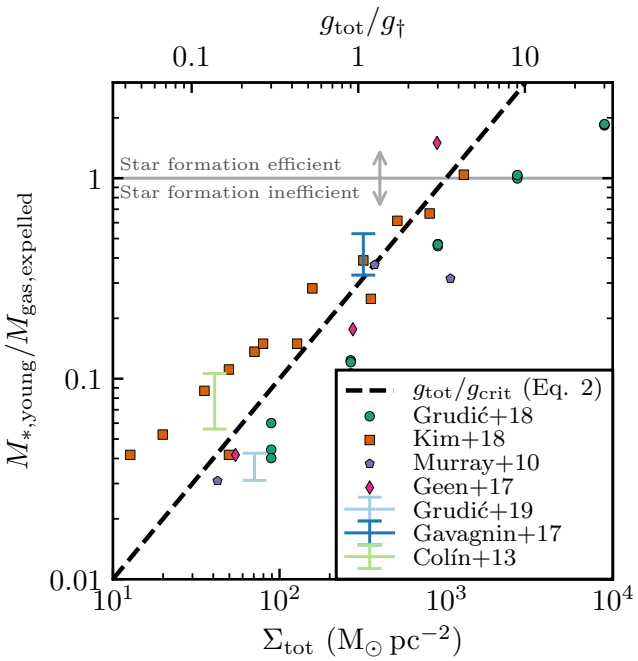

Figure 1. Ratio of the young stellar mass formed to the expelled gas mass in GMCs predicted by different theoretical models as a function of total mass surface density $\Sigma_{\rm tot}$, which is equivalent to an effective acceleration $g_{\rm tot} \equiv \pi G \Sigma_{\rm tot}$, plotted on top in units of $g_\dagger$ (the observed characteristic acceleration scale of galaxies). The dashed line shows the simple analytic scaling from Eq. 2 for comparison. All the models predict that $M_{*,\rm young}/M_{\rm expelled} \rightarrow 1$ as $\Sigma_{\rm tot}$ exceeds $\Sigma_{\rm crit} \sim 10^3\,\rm M_\odot\,pc^{-2}$, i.e. star formation becomes efficient. These results come primarily from (magneto)hydrodynamic simulations (Colín et al. 2013; Geen et al. 2017; Gavagnin et al. 2017; Grudić et al. 2018; Kim et al. 2018; Grudić et al. 2019), and all include stellar feedback at least in the form of radiation from massive stars. The Murray et al. (2010) results are based on semi-analytic calculations. Error bars denote the full range of results obtained in studies that survey only one value of $\Sigma_{\rm eff}$ and vary either cloud mass or physics prescriptions.

to its dark matter halo and that this connection must be in some sense "universal." Any successful and predictive explanation within ΛCDM (or any extension) must explain the origin and numerical value of the critical acceleration scale $g_\dagger$. In this Letter, we argue that stellar feedback in the form of momentum injection from massive stars naturally explains the critical acceleration scale found in observations of disk galaxies, with that scale *built in* to stellar physics and evolution as opposed to arising from a coincidence or "fine-tuning" of various effects.

2 PHYSICAL MODEL

2.1 Scaling of the Star Formation Efficiency

The scaling of the star formation efficiency as a competition between gravity and stellar feedback has been extensively studied over the last few decades, both in the context of individual star-forming clouds and for entire galaxies (e.g. Larson 1974; Rees & Ostriker 1977; Dekel & Silk 1986; Silk 1997; Efstathiou 2000; Murray et al. 2005, 2010; Fall et al. 2010). Below we sketch a simplified derivation that captures the core of our present understanding of self-regulated star formation.

Consider a "patch" of gas in a galactic disk (or cloud) of mass $M_{\rm gas,initial}$ and area $A \sim \pi R^2$ which is Jeans unstable and begins to cool and form stars. These stars will act back on the collapsing gas, injecting momentum at a rate per unit area $d\dot{P}_{\rm fb}/dA$ which is proportional to the mass of young stars (since the feedback is dominated by massive stars), $d\dot{P}_{\rm fb}/dA \sim \langle \dot{p}/m_* \rangle\, M_{*,\rm young}/A$ (where $\langle \dot{p}/m_* \rangle$ is the momentum injection rate per stellar mass formed). If this exceeds the force per unit area on the gas from gravity $\sim \pi G\, M_{\rm tot}\, M_{\rm gas}/R^4 = \pi G \Sigma_{\rm gas} \Sigma_{\rm tot}$, then the weight of the gas column is unbound, i.e. SF ceases and gas is ejected when

$$\frac{M_{*,\rm young}}{M_{\rm gas,expelled}} \sim \frac{\pi\, G\, M_{\rm tot}}{\langle \dot{p}/m_* \rangle\, R^2} = \frac{\Sigma_{\rm tot}}{\Sigma_{\rm crit}} \qquad (1)$$

where $\Sigma_{\rm tot} \equiv M_{\rm tot}/A$ and $\Sigma_{\rm crit} \equiv \langle \dot{p}/m_* \rangle/(\pi^2\, G)$.

In the last few years, a considerable body of work has explored the SFE and demonstrated that such a scaling, with a roughly constant $\Sigma_{\rm crit} \sim 1000\,\rm M_\odot\,pc^{-2}$, works remarkably well at describing both observations (e.g., Wong et al. 2019) and detailed numerical simulations of cloud collapse (e.g., Hopkins et al. 2012a; Colín et al. 2013; Raskutti et al. 2016; Gavagnin et al. 2017; Grudić et al. 2018; Hopkins & Grudić 2018; Kim et al. 2018; Li et al. 2019). We compile in Figure 1 SFE predictions for GMCs from various simulations that include stellar feedback. The compilation shows that there is an emerging consensus that the SFE scales linearly with $\Sigma_{\rm tot}$ over at least two orders of magnitude in surface density, reaching ~ 1 for $\Sigma_{\rm tot} \gtrsim \Sigma_{\rm crit}$.[1] Although the model predictions vary at the factor $\sim 2-3$ level at fixed $\Sigma_{\rm tot}$, much of the scatter can be attributed to differences in initial conditions, definitions, and numerical methods (e.g., Hopkins & Grudić 2018; Geen et al. 2018; Grudić & Hopkins 2019).

Moreover, the ensemble and time-averaged version of this simple scaling can explain the observed Schmidt-Kennicutt relation in terms of $\langle \dot{p}/m_* \rangle$ (or its time-integrated-equivalent $\langle p/m_* \rangle$; e.g., Silk 1997; Thompson et al. 2005; Ostriker & Shetty 2011; Hopkins et al. 2011; Faucher-Giguère et al. 2013; Semenov et al. 2016; Orr et al. 2018). Taken one step further, this also naturally leads to the scalings for momentum-conserving galactic outflows (e.g., Murray et al. 2005; Hopkins et al. 2012b; Hayward & Hopkins 2017), with the same constant $\langle \dot{p}/m_* \rangle$ appearing.[2]

The value $\langle \dot{p}/m_* \rangle$ thus plays a critical and "universal" role in star formation. It is important to note that

[1] It is common in the star formation literature to define the SFE as $M_{*,\rm young}/(M_{\rm gas,expelled} + M_{*,\rm young})$, effectively neglecting the possibility of a significant dark matter component.

[2] If instead of the non-equilibrium derivation of Eq. (1), one considers a time-steady galactic SFR $\dot{M}_*$ and wind mass loss $\dot{M}_{\rm out}$ with momentum flux $\dot{M}_{\rm out}\, v_{\rm escape} \sim \langle p/m_* \rangle \dot{M}_* \sim \langle \dot{p}/m_* \rangle\, M_{*,\rm young}$ (where $\langle p/m_* \rangle = \int \langle \dot{p}/m_* \rangle\, dt \sim t_* \langle \dot{p}/m_* \rangle$ for a single stellar population), one obtains the usual momentum-driven wind scaling $\dot{M}_{\rm out} \propto 1/v_{\rm escape}$ (e.g., Murray et al. 2005; Davé et al. 2011) and we can write $M_*/M_{\rm gas,expelled} \sim \langle \dot{M}_* \rangle/\langle \dot{M}_{\rm out} \rangle \sim v_{\rm escape}/\langle p/m_* \rangle \sim (t_*\,\Omega)^{-1}\,(g_{\rm tot}/g_{\rm crit})$, where $t_*\,\Omega \sim 1$ is a correction applicable when $\Omega^{-1} \gtrsim t_*$.

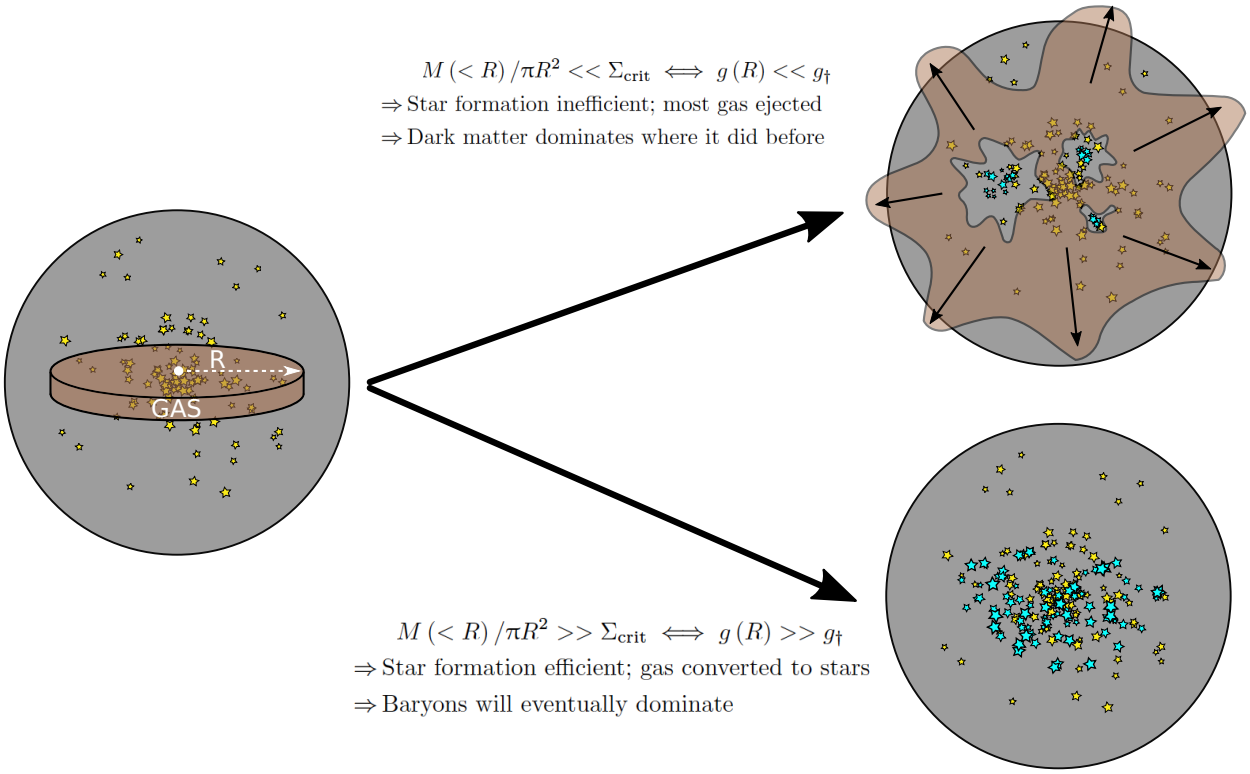

Figure 2. Illustration of the two opposite limiting behaviours of a star-forming patch of gas localized within a radius R within a galaxy, as determined by the acceleration (or equivalently, mass surface density) scale according to the physical arguments in §2.1. If $\Sigma_{\rm tot} \equiv M\,(<R)\,/\pi R^2 \ll \Sigma_{\rm crit}$ (or equivalently, $g_{\rm tot}\,(R) \ll g_\dagger$), star formation will be inefficient, most gas mass will be ejected, and dark matter will continue to dominate where it did before. If $\Sigma_{\rm tot} \gg \Sigma_{\rm crit}$ (or equivalently, $g_{\rm tot}\,(R) \gg g_\dagger$), star formation will be efficient, and baryonic matter will eventually dominate. As a result, $g_\dagger$ demarcates the transition from baryon- to dark matter-dominated regions.

the value of $\langle \dot{p}/m_* \rangle$ is similar regardless of whether photo-heating, radiation pressure, stellar OB winds, or supernovae (SNe) dominate the feedback, as they all provide similar momentum injection rates for standard stellar population models (e.g., Leitherer et al. 1999; Bruzual & Charlot 2003; Agertz et al. 2013; Hopkins et al. 2011). For example, radiative feedback provides $\langle \dot{p}/m_* \rangle \sim c^{-1}\,(L/M)_{*,\,\rm young} \sim c^{-1}\,(1000\,L_\odot/M_\odot) \sim 1000$ km s^{-1}/40 Myr while SNe, which release their momentum over a stellar evolution timescale $t_* \sim 40$ Myr, also output $\langle \dot{p}/m_* \rangle \approx 1000$ km s^{-1}/40 Myr, nearly independent of ambient medium properties (e.g., Martizzi et al. 2015; Kim & Ostriker 2015).

For these reasons, although controversy and unsolved questions still remain in the study of star formation and details of e.g. Eq. 1, this controversy has largely centered on the exact order-unity coefficients (e.g. fraction of the momentum coupled vs. "vented," corrections for turbulent media, and non-linear time-dependent effects), and question of which feedback mechanisms dominate on which spatial and timescales (none of which alters the dimensional scaling in Eq. 1).

2.2 A Characteristic Acceleration Scale from Stellar Feedback

For historical reasons, the convention in the star formation literature has been to express Eq. 1 in terms of a critical surface density and it is common to assume (e.g., in the context of individual molecular clouds) that $\Sigma_{\rm tot}$ is dominated by baryons. However, the derivation in the previous section shows that the relevant quantity is actually the total gravitational acceleration from all matter, $g_{\rm tot} = G\,M_{\rm tot}/r^2$. Noting this, Eq. 1 can be rewritten as

$$\frac{M_{*,\,\rm young}}{M_{\rm gas,\,expelled}} \sim \frac{\pi\,G\,M_{\rm tot}}{\langle \dot{p}/m_* \rangle\,R^2} = \frac{g_{\rm tot}}{g_{\rm crit}} \qquad (2)$$

$$g_{\rm crit} \equiv \frac{1}{\pi}\,\langle \dot{p}/m_* \rangle = \pi\,G\,\Sigma_{\rm crit} \sim 2\times10^{-8}\ {\rm cm\,s^{-2}} \sim {\rm g}_\dagger.$$

Expressed in cgs units, we see that $g_{\rm crit} \sim 0.3\,\langle \dot{p}/m_* \rangle$ corresponds numerically to the "universal" acceleration $g_\dagger$ of galaxies.

Consider now what happens in different limits of the gravitational acceleration, as implied by Eq. 2 and illustrated in Figure 2. If $g_{\rm tot} \ll g_{\rm crit}$, then $M_{*,\,\rm young}/M_{\rm gas,\,expelled} \ll 1$ and the fraction of the total gas mass converted to stars is small. Thus, if dark matter initially dominates $M_{\rm tot}\,(<R)$, it will generally continue to do so. In the opposite limit, where $g_{\rm tot} \gg g_{\rm crit}$, the SFE is high and baryons cannot escape the galaxy. In such an instance, where feedback is ineffective, dissipative gas accretion within dark matter halos is easily sufficient to allow baryonic matter to dominate over dark matter (Fall & Efstathiou 1980; Katz et al. 1996). As a result, $g_{\rm crit} \sim g_\dagger$ will demarcate the transition between the baryon-dominated and dark matter-dominated regions of a galaxy.

2.3 Accelerations in the Dark Matter-Dominated ("Deep-MOND") Limit & Flat Rotation Curves

In the previous section we argued that, at large accelerations $g_{\rm tot} \gg g_\dagger$, the total mass is expected to be dominated by baryons and therefore $g_{\rm tot} \equiv G\,M_{\rm tot}(<r)/r^2 \approx g_{\rm baryon} \equiv GM_{\rm bar}(<r)/r^2$ (where $M_{\rm bar}(<r)$ is the baryonic mass enclosed in r), as is indeed observed. We now consider in more detail the low-acceleration ("deep MOND") regime, $g_{\rm tot} \ll g_\dagger$. In this regime (corresponding to large galacto-centric distances in normal galaxies, and all radii in many dwarf and low-surface brightness galaxies), the accelerations are observed to scale approximately as $g_{\rm tot} \approx (g_{\rm baryon}\, g_\dagger)^{1/2}$ (e.g. Lelli et al. 2017). Equivalently (since $g_{\rm tot} \equiv V_c^2/r$ in terms of the circular velocity V_c), $V_c \approx (GM_{\rm bar}(<r)\, g_\dagger)^{1/4}$ – i.e. rotation curves are asymptotically "flat" ($V_c \rightarrow$ constant as $r \rightarrow \infty$) with a universal scale $g_\dagger$ above which $g_{\rm tot} \approx g_{\rm baryon}$. This classic result, which is generally interpreted as evidence for dark matter, was a key motivation for introducing MOND; rather than assuming Newtonian gravity with $g_{\rm tot} = g_{\rm Newtonian} = GM_{\rm tot}/r^2$ at $g_{\rm tot} \ll g_\dagger$ (requiring $M_{\rm tot} \gg M_{\rm bar}$, i.e. dark matter), Milgrom (1983a) proposed $M_{\rm tot} = M_{\rm bar}$, but with a modified acceleration law $g_{\rm tot} \rightarrow g_{\rm MOND} = (g_{\rm Newtonian} g_\dagger)^{1/2} = (g_\dagger\, GM_{\rm bar}(<r)/r^2)^{1/2}$ when $g_{\rm tot} \ll g_\dagger$.

But in the limit $g_{\rm tot} \ll g_\dagger$, our Eq. 2 implies that the stellar mass $M_* \sim (g_{\rm tot}/g_{\rm crit})\, M_{\rm gas,\,initial} \approx (g_{\rm tot}/g_{\rm crit}) f_{\rm bar}^0 M_{\rm tot}$, where $f_{\rm bar}^0 \equiv M_{\rm gas,\,initial}/M_{\rm tot}$ refers to the initial "total" supply of baryons.[3] Solving for the total mass,

$$M_{\rm tot}(<r) \approx \left(\frac{g_{\rm crit}}{g_{\rm tot}}\right) \frac{M_*(<r)}{f_{\rm bar}^0} \approx \left(\frac{g_{\rm crit}}{g_{\rm tot}}\right) \frac{(1-f_{\rm g})}{f_{\rm bar}^0} M_{\rm bar}(<r), \quad (3)$$

where $f_{\rm g} = M_{\rm gas}^{\rm relic}/(M_{\rm gas}^{\rm relic} + M_*)$ is the gas fraction determined by the "relic" gas mass $M_{\rm gas}^{\rm relic}$ that remains after expulsion by stellar feedback. Using the above relations, standard Newtonian dynamics imply that the total acceleration $g_{\rm tot} = g_{\rm Newtonian}$ is:

$$g_{\rm tot} \approx \frac{GM_{\rm tot}(<r)}{r^2} \approx \left(\frac{g_{\rm crit}}{g_{\rm tot}}\right) \frac{(1-f_{\rm g})}{f_{\rm bar}^0} \frac{GM_{\rm bar}(<r)}{r^2} = \left(\frac{\tilde{g}_{\rm crit}}{g_{\rm tot}}\right) g_{\rm baryon} \quad (4)$$

$$\Rightarrow g_{\rm tot} \approx \left(g_{\rm baryon}\, \tilde{g}_{\rm crit}\right)^{1/2}, \quad (5)$$

where $\tilde{g}_{\rm crit} \equiv g_{\rm crit}(1-f_{\rm g})/f_{\rm bar}^0$ only differs from $g_{\rm crit}$ at the order unity level. Identifying $\tilde{g}_{\rm crit}$ with $g_\dagger$, this is exactly the scaling observed.

Thus, not only the characteristic acceleration $g_\dagger$, *but also* the asymptotic scalings at both low and high accelerations that define the observed RAR (and MOND, by construction) emerge naturally. Equivalently, the fact that observed rotation curves are approximately flat at large radii does not require a "conspiracy" or "coincidence" between baryons and dark matter: rather, stellar feedback ensures the baryons self-regulate with the scaling needed to ensure approximately flat V_c.[4] In modern parlance, Eq. 2 predicts a stellar mass-halo mass relation at low masses of $M_* \sim (g_{\rm tot}/g_{\rm crit})\, M_{\rm gas,\,initial} \propto M_{\rm tot}^2$ (since $g_{\rm tot}$ and $M_{\rm gas,\,initial} \propto M_{\rm tot}$ while $g_{\rm crit}$ is constant), in good agreement with the relation observed and needed to reproduce *both* the galaxy luminosity functions and the baryonic Tully-Fisher relation (e.g., McGaugh et al. 2000; Moster et al. 2010; Behroozi et al. 2013). This in turn leads automatically to the observed RAR (Wheeler et al. 2018).

2.4 Expressing $g_\dagger$ in Fundamental Constants

According to the picture proposed here, $g_\dagger \sim g_{\rm crit} \sim 0.3\,\langle \dot{p}/m_* \rangle$. But $\langle \dot{p}/m_* \rangle$ itself can be understood in terms of the stellar IMF and the physics of massive stars. As discussed in §2.1, the stellar population-averaged $\dot{p} \sim L/c$ (i.e. $\langle \dot{p}/m_* \rangle \sim c^{-1}\,(L/M)_{*,\,\rm young}$) for a variety of feedback mechanisms, and the most massive stars dominate the luminosity and feedback. The luminosities of these stars are set by the Eddington limit:

$$L_{\rm Edd,\,i} = \frac{4\pi G m_{\rm p} c}{\sigma_{\rm T}} M_i, \quad (6)$$

where M_i is the mass of an individual massive star and $\sigma_{\rm T}$ is the Thomson cross-section. So $(L/M)_{*,\,\rm young} \sim f_{\rm massive}\, L_{\rm Edd,\,i}/M_i$ where the $f_{\rm massive}$ is the mass fraction in massive stars: to reproduce the more accurate full stellar population calculation for a standard IMF (Leitherer et al. 1999), $f_{\rm massive} \sim 0.03$.[5] Thus we have $\langle \dot{p}/m_* \rangle \sim f_{\rm massive}\,(4\pi\, G\, m_{\rm p})/\sigma_{\rm T}$. Putting these together, we obtain:

$$g_\dagger \sim g_{\rm crit} \sim (4\, f_{\rm massive})\, \frac{Gm_{\rm p}}{\sigma_{\rm T}} \sim 0.1\, \frac{Gm_{\rm p}}{\sigma_{\rm T}} \sim 0.5\, Gm_{\rm p} \left(\frac{m_{\rm e} c}{\alpha h}\right)^2, \quad (7)$$

where the last expression uses $\sigma_{\rm T} \equiv \frac{8\pi}{3}\left(\frac{\alpha \hbar c}{m_{\rm e} c^2}\right)^2$, in terms of the fine-structure constant α, the Planck constant $\hbar = h/2\pi$, the electron mass m_e, and the speed of light c.

3 DISCUSSION

3.1 Departures from universality

Recent observational analyses have cast serious doubt upon a *fundamental* RAR to which all galaxies must conform exactly (Rodrigues et al. 2018; Stone & Courteau 2019; Chang & Zhou 2019), contrary to previous claims that the observed scatter is fully consistent with measurement error. Hence, whatever the origin of $g_\dagger$, it is likely emergent rather than fundamental in nature. This fits with the picture presented in this paper: although $g_{\rm crit}$ sets a characteristic scale, there is no reason why galaxies should conform *exactly* to a single RAR. For example, galaxy formation is the product of both in-situ star formation and hierarchical merging (e.g.,

[3] Since the SFE is low in this regime, the expelled gas mass is close to the total initial gas mass.

[4] We note the factor $(1-f_{\rm g})/f_{\rm bar}^0$ is not exactly constant at large radii (though for e.g. a galaxy in a Navarro et al. 1996b dark matter halo it varies extremely weakly with radius): this reflects the fact that rotation curves are not perfectly flat (e.g., Salucci & Burkert 2000; Courteau & Dutton 2015).

[5] Krumholz (2011) argue that the form of the IMF, and by extension $f_{\rm massive}$, are also expressible in terms of fundamental constants.

Anglés-Alcázar et al. 2017), with merging becoming increasingly important at higher masses, e.g. for massive elliptical galaxies. Feedback from active galactic nuclei (AGN), rather than stars, is also expected to be most important in massive galaxies. Interestingly, while lower-mass disk galaxies prefer the characteristic acceleration described here, the massive elliptical do not (though they do preserve "memory" of the mass profiles of merged galaxies; see Boylan-Kolchin et al. 2005). Thus, effects like variations in galaxy assembly history and AGN feedback might drive scatter in the RAR and rotation curve shapes.

3.2 Effect of IMF variations

Another source of scatter would be variations in the stellar IMF: $\dot{p}/m_*$ is sensitive to the massive stellar content of a stellar population, so within a given galaxy the observed $g_\dagger$ should vary with it accordingly. *Random* variations in $f_{\rm massive}$ are present in any stellar population "sampled" from an IMF due to the finite number of stars, but in particular the effect of "incomplete" sampling of the IMF upon $\dot{p}/m_*$ becomes pronounced for stellar populations less massive than $10^4 M_\odot$ (Murray & Rahman 2010; Kim et al. 2016). We thus expect increased scatter in the BTFR and RAR in ultra-faint dwarf (UFD) galaxies with $M_* < 10^4 M_\odot$.

It is also possible for the IMF to vary systematically from one galaxy to another, and $g_\dagger$ with it. However, the factor $f_{\rm massive}$ is fairly well-constrained in an average sense: if it varied strongly with galaxy or local environmental properties, the slopes and normalizations of the Schmidt-Kennicutt and $M_* - M_{\rm halo}$ relations would be quite different. Furthermore, direct observations are consistent with an IMF that is common to all galaxies (Bastian et al. 2010; Offner et al. 2014). Therefore, while variations in the measured $g_\dagger$ could conceivably be driven by IMF variations, it seems likely that they would be dominated by other sources of variations, such as galactic environment and assembly history. Insofar as the IMF *is* roughly universal across cosmic time and feedback does not depend strongly on factors such as metallicity, the arguments presented above imply that (1) the characteristic acceleration scale should not vary systematically with redshift and (2) the observation that $g_\dagger \approx c\,H_0$ in the low-redshift Universe (Milgrom 1983a) is a numerical coincidence.

3.3 Additional Details in Cosmological Calculations

In ΛCDM, dark-matter-only simulations predict NFW-like dark matter profiles with $\rho \propto r^{-1}$ on small scales. In such halos, the maximum (central) acceleration is nearly constant, $g_{\rm tot}^{\rm cen} \sim 3\times10^{-9}\ {\rm cm\,s^{-2}}$ (or central $\Sigma_{\rm DM}^{\rm cen} \sim 100\,M_\odot\,{\rm pc^{-2}} < \Sigma_{\rm crit}$), with very weak dependence on halo mass and/or redshift, although the presence of baryons and stellar feedback can strongly alter this (e.g. Navarro et al. 1996a; Governato et al. 2010; Oñorbe et al. 2015). A "pure" dark halo therefore has $g_{\rm tot} \lesssim g_{\rm crit}$ at all radii.[6] But if all of the available baryons fall in, conservation of specific angular momentum implies circularization in a disk with extent $r \sim \lambda\,R_{\rm vir}$ (where $R_{\rm vir}$ is the virial radius; e.g., Fall & Efstathiou 1980; Mo et al. 1998). The acceleration in the galaxy $g_{\rm tot} \sim 2\times10^{-8}\,(1+z)^2\ {\rm cm\,s^{-2}}$ ($\Sigma_{\rm bar} \sim 500\,(1+z)^2\,M_\odot\,{\rm pc^{-2}}$) then approaches the critical value. There are therefore several ways that halo centers can become strongly baryon-dominated: (a) most of the baryons fall in by $z = 0$, (b) a smaller fraction of baryons fall in at high redshift, or (c) the baryons lose angular momentum and more efficiently sink to the center.

Properly accounting for the complexities of galaxy formation requires much more detailed modeling. But of course, this is what cosmological simulations and semi-analytic models do. These calculations have indeed shown that the characteristic acceleration scale $g_\dagger$, and more detailed scaling relations such as the RAR and baryonic Tully-Fisher relation (BTFR), emerge naturally in ΛCDM *provided* the models accurately treat stellar feedback (e.g. Navarro et al. 2017; Ludlow et al. 2017; Keller & Wadsley 2017; Dutton et al. 2019). More specifically, previous studies have shown that in ΛCDM models that produce the "correct" galaxy sizes and masses, the characteristic $g_\dagger$ appears in rotation curves as observed; Wheeler et al. (2018) showed more explicitly that as long as galaxies are broadly consistent with the observed BTFR, this is essentially guaranteed. And it is well known that stellar feedback with $\langle \dot{p}/m_* \rangle$ similar to the values assumed here, based on standard stellar evolution models, is necessary to reproduce these scaling relations in ΛCDM (e.g., Somerville & Davé 2015). The simple arguments presented in this paper do not supplant these much more detailed and sophisticated calculations. Rather, they help demonstrate that the observed universal acceleration scale of galaxies does not require a "conspiracy" between many different fine-tuned components nor a modified theory of gravity: *stellar feedback explicitly contains an acceleration scale* that maps directly to the acceleration scale seen in galaxy scaling relations.

[6] This alone can explain, in part, why systems with $g_{\rm tot} \gg g_\dagger$ must be baryon-dominated, but it does not explain why systems with $g_{\rm tot} \ll g_\dagger$ could not also be baryon-dominated.

ACKNOWLEDGEMENTS

We thank Jonathan Stern for useful discussions and for proposing ideas explored in §2.3. MYG is supported by the CIERA Postdoctoral Fellowship Program. MBK acknowledges support from NSF grants AST-1517226, AST-1910346 and CAREER award AST-1752913, NASA grant NNX17AG29G and grants HST-AR-13888, HST-AR-13896, HST-AR-14282, HST-AR-14554, HST-AR-15006, HST-GO-12914, and HST-GO-14191 from the Space Telescope Science Institute, which is operated by AURA, Inc., under NASA contract NAS5-26555. CAFG is supported by NSF through grants AST-1517491, AST-1715216, and CAREER award AST-1652522, by NASA through grant 17-ATP17-0067, and by a Cottrell Scholar Award from the Research Corporation for Science Advancement. Support for PFH was provided by an Alfred P. Sloan Research Fellowship, NSF Collaborative Research Grant #1715847 and CAREER grant #1455342, and NASA grants NNX15AT06G, JPL 1589742, and 17-ATP17-0214.

REFERENCES

Agertz O., Kravtsov A. V., Leitner S. N., Gnedin N. Y., 2013, ApJ, 770, 25
Anglés-Alcázar D., Faucher-Giguère C.-A., Kereš D., Hopkins P. F., Quataert E., Murray N., 2017, MNRAS, 470, 4698
Bastian N., Covey K. R., Meyer M. R., 2010, ARA&A, 48, 339
Behroozi P. S., Wechsler R. H., Conroy C., 2013, ApJ, 770, 57
Bershady M. A., Martinsson T. P. K., Verheijen M. A. W., Westfall K. B., Andersen D. R., Swaters R. A., 2011, ApJ, 739, L47
Bosma A., 1981a, AJ, 86, 1791
Bosma A., 1981b, AJ, 86, 1825
Boylan-Kolchin M., Ma C.-P., Quataert E., 2005, MNRAS, 362, 184
Bruzual G., Charlot S., 2003, MNRAS, 344, 1000
Chang Z., Zhou Y., 2019, MNRAS, 486, 1658
Colín P., Vázquez-Semadeni E., Gómez G. C., 2013, MNRAS, 435, 1701
Courteau S., Dutton A. A., 2015, ApJ, 801, L20
Davé R., Oppenheimer B. D., Finlator K., 2011, MNRAS, 415, 11
Dekel A., Silk J., 1986, ApJ, 303, 39
Dutton A. A., Macciò A. V., Obreja A., Buck T., 2019, MNRAS, 485, 1886
Efstathiou G., 2000, MNRAS, 317, 697
Fall S. M., Efstathiou G., 1980, MNRAS, 193, 189
Fall S. M., Krumholz M. R., Matzner C. D., 2010, ApJ, 710, L142
Faucher-Giguère C.-A., Quataert E., Hopkins P. F., 2013, MNRAS, 433, 1970
Gavagnin E., Bleuler A., Rosdahl J., Teyssier R., 2017, MNRAS, 472, 4155
Geen S., Soler J. D., Hennebelle P., 2017, MNRAS, 471, 4844
Geen S., Watson S. K., Rosdahl J., Bieri R., Klessen R. S., Hennebelle P., 2018, MNRAS, 481, 2548
Governato F., et al., 2010, Nature, 463, 203
Grudić M. Y., Hopkins P. F., 2019, MNRAS, 488, 2970
Grudić M. Y., Hopkins P. F., Faucher-Giguère C.-A., Quataert E., Murray N., Kereš D., 2018, MNRAS, 475, 3511
Grudić M. Y., Hopkins P. F., Lee E. J., Murray N., Faucher-Giguère C.-A., Johnson L. C., 2019, MNRAS, 488, 1501
Hayward C. C., Hopkins P. F., 2017, MNRAS, 465, 1682
Hopkins P. F., Grudić M. Y., 2018, preprint, (arXiv:1803.07573)
Hopkins P. F., Quataert E., Murray N., 2011, MNRAS, 417, 950
Hopkins P. F., Quataert E., Murray N., 2012a, MNRAS, 421, 3488
Hopkins P. F., Quataert E., Murray N., 2012b, MNRAS, 421, 3522
Katz N., Weinberg D. H., Hernquist L., 1996, ApJS, 105, 19
Keller B. W., Wadsley J. W., 2017, ApJ, 835, L17
Kim C.-G., Ostriker E. C., 2015, ApJ, 802, 99
Kim J.-G., Kim W.-T., Ostriker E. C., 2016, ApJ, 819, 137
Kim J.-G., Kim W.-T., Ostriker E. C., 2018, ApJ, 859, 68
Krumholz M. R., 2011, The Astrophysical Journal, 743, 110
Larson R. B., 1974, MNRAS, 169, 229
Leitherer C., et al., 1999, ApJS, 123, 3
Lelli F., McGaugh S. S., Schombert J. M., Pawlowski M. S., 2017, ApJ, 836, 152
Li H., Vogelsberger M., Marinacci F., Gnedin O. Y., 2019, arXiv e-prints, p. arXiv:1904.11987
Ludlow A. D., et al., 2017, Phys. Rev. Lett., 118, 161103
Martizzi D., Faucher-Giguère C.-A., Quataert E., 2015, MNRAS, 450, 504
McGaugh S. S., Schombert J. M., Bothun G. D., de Blok W. J. G., 2000, ApJ, 533, L99
Milgrom M., 1983a, ApJ, 270, 365
Milgrom M., 1983b, ApJ, 270, 371
Milgrom M., 1983c, ApJ, 270, 384
Mo H. J., Mao S., White S. D. M., 1998, MNRAS, 295, 319
Moster B. P., Somerville R. S., Maulbetsch C., van den Bosch F. C., Macciò A. V., Naab T., Oser L., 2010, ApJ, 710, 903
Murray N., Rahman M., 2010, ApJ, 709, 424
Murray N., Quataert E., Thompson T. A., 2005, ApJ, 618, 569
Murray N., Quataert E., Thompson T. A., 2010, ApJ, 709, 191
Navarro J. F., Eke V. R., Frenk C. S., 1996a, MNRAS, 283, L72
Navarro J. F., Frenk C. S., White S. D. M., 1996b, ApJ, 462, 563
Navarro J. F., Benítez-Llambay A., Fattahi A., Frenk C. S., Ludlow A. D., Oman K. A., Schaller M., Theuns T., 2017, MNRAS, 471, 1841
Oñorbe J., Boylan-Kolchin M., Bullock J. S., Hopkins P. F., Kereš D., Faucher-Giguère C.-A., Quataert E., Murray N., 2015, MNRAS, 454, 2092
Offner S. S. R., Clark P. C., Hennebelle P., Bastian N., Bate M. R., Hopkins P. F., Moraux E., Whitworth A. P., 2014, Protostars and Planets VI, pp 53–75
Orr M. E., et al., 2018, MNRAS, 478, 3653
Ostriker E. C., Shetty R., 2011, ApJ, 731, 41
Planck Collaboration et al., 2018, arXiv e-prints, p. arXiv:1807.06209
Raskutti S., Ostriker E. C., Skinner M. A., 2016, ApJ, 829, 130
Rees M. J., Ostriker J. P., 1977, MNRAS, 179, 541
Rodrigues D. C., Marra V., del Popolo A., Davari Z., 2018, Nature Astronomy, 2, 668
Rubin V. C., Ford Jr. W. K., Thonnard N., 1978, ApJ, 225, L107
Rubin V. C., Ford Jr. W. K., Thonnard N., 1980, ApJ, 238, 471
Salucci P., Burkert A., 2000, ApJ, 537, L9
Semenov V. A., Kravtsov A. V., Gnedin N. Y., 2016, ApJ, 826, 200
Silk J., 1997, ApJ, 481, 703
Somerville R. S., Davé R., 2015, ARA&A, 53, 51
Stone C., Courteau S., 2019, ApJ, 882, 6
Thompson T. A., Quataert E., Murray N., 2005, ApJ, 630, 167
Wheeler C., Hopkins P. F., Doré O., 2018, arXiv e-prints, p. arXiv:1803.01849
Wong T., et al., 2019, arXiv e-prints, p. arXiv:1905.11827

This paper has been typeset from a TEX/LATEX file prepared by the author.